Study of large-scale deformation induced by gravity on the La Clapière landslide (Saint-Etienne de Tinée, France) using numerical and geophysical approaches

E. Tric *, T. Lebourg, H. Jomard, J. Le Cossec

Laboratoire Géoazur, Université de Nice — Sophia Antipolis, CNRS/ IRD, Observatoire de la Côte d'Azur, 250 rue A. Einstein, 06560 Valbonne, France

ARTICLE INFO

ABSTRACT

The large-scale deformation of high mountain slopes finds its origin in many phenomena with very different time-constants. Gravitational effect, tectonic forces, and water infiltration are generally the principal causes. However, it is always very difficult to distinguish which cause is dominant and which are their respective effects. A two-dimensional numerical experiment coupled with geophysical approach was carried out to determine (1) the effect of gravitational force on the mechanical behaviour of the "la Clapière" area, (2) a 2D-depth structure of this landslide. The results show that gravitational instability is possible and leads to destabilisation of the massif by a regressive evolution of the landslide from the bottom at 1100 m up to a height of 1800 m, which is actually the top of the La Clapière landslide. This deformation progression only concerns a depth of around 150 ± 50 m, which can be correlated to the sliding surface, as suggested by our electrical data obtained by resistivity investigations and previous studies. Our numerical results suggest that changes of the slope topography "drive" the diffusion of the plastic deformation in the mass, possibly through a channel which could be then the privileged zone along which the fracture is initiated.

1. Introduction

For the study of the deformation or the stability analysis of high mountain slopes, knowledge of the large-scale mechanical properties is important. Different approaches exist to estimate those parameters, such as seismic measurements (Eberhardt-Philips et al., 1995; Brueckl and Parotidis, 2001), geotechnical measurements, such as the "Schmidt hammer tests" (Bieniawski, 1989; Gunzburger, 2001; Gunzburger and Merrien-Soukatchoff, 2002; Aydin and Basu, 2005) or mechanical tests in the laboratory (Lebourg et al., 2004). However, these different observational analyses do not have the potential to reveal the processes involved in the generation and development of a creeping rock mass from an originally compact rock. A promising addition could be geomechanical modelling of the structures of the creeping or sliding rock masses. Thus, geomechanical parameters may be determined by fitting the geomechanical model to the structures as determined from geophysical exploration (seismic or electrical). This approach, rapidly evolving due to increasing computer power, also allows definition of the stress–strain state of the slope with use of the relevant non-linear mathematical models of the soils and rigorous consideration of all acting forces as well as the variation of mechanical properties with depth (Savage et al., 2000; Brueckl and Parotidis, 2001; Merrien-Soukatchoff et al., 2001; Eberhardt et al., 2004; Maffei et al., 2005).

In this contribution, we present an application of the numerical approach to the "La Clapière" landslide (Alpes-Maritimes, France). Indeed, while numerous studies have been carried out on this site (hydrological, geologic, tectonic, topographic, etc.) (Follacci, 1987; Ivaldi et al., 1991; Compagnon et al., 1997; Guglielmi et al., 2000, 2002; Gunzburger and Laumonier, 2002), very few numerical studies have been conducted (Quenot, 2000; Merrien-Soukatchoff et al., 2001; Gunzburger et al., 2002; Cappa et al., 2004) and, to our knowledge, no study has been devoted to the localisation of the deformation as a function of the geomechanical parameters and their relation to the gravitational destabilisation of the slope. In the second part of this contribution, we present the comparison between our numerical data and an electrical survey that we have conducted on the La Clapière landslide and previous results obtained by our team (Lebourg et al., 2005; Jomard et al., 2007a).

2. The "La Clapière" landslide

The "La Clapière" landslide is a large unstable slope located in south-eastern France, in the Alps, about 80 km north of the city of Nice. This landslide which mobilizes a huge volume (55×510^6 m^3) of metamorphic rocks in the Mercantour massif (Follacci, 1999) has developed on the left bank of Tinee Valley and affects a slope that culminates at 3000 m, between 1100 and 1800 m in altitude (Fig. 1). It is bordered on its north-western side by the Tenibres River and to its south-eastern side by the Rabuons River, flowing into the Tinée River. A large rupture has been identified since the beginning of the century: in 1936 the wrenching at the top of the landslide was already quite
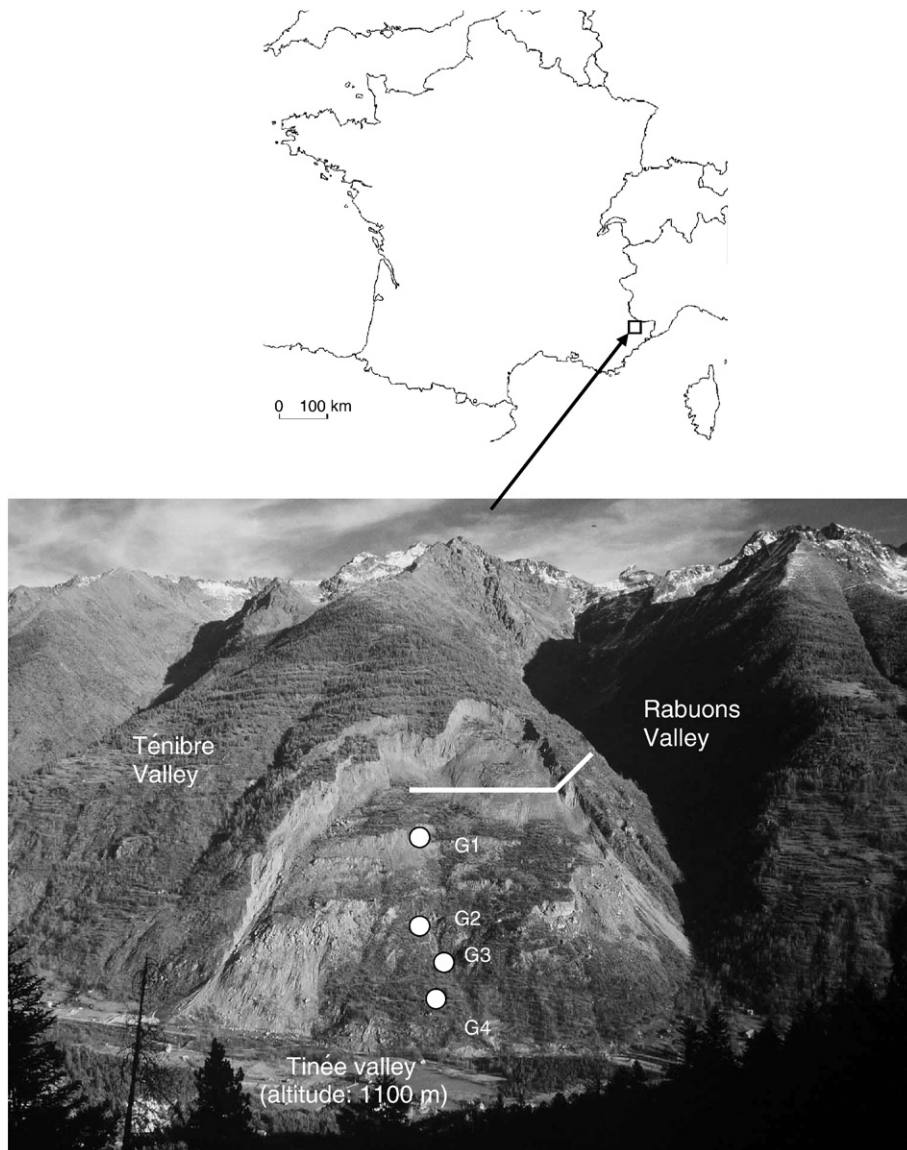
Fig. 1. The "La Clapière" landslide in 1998 (View from CETE de Nice). The location of the SEV Schlumberger array (dots G1, G2, G3 and G4) and tomography profile (line) which have been carried out on the La Clapière landslide are given on the photography.

visible. In the 1970s, the movements became more continuous and monitoring of the site has been in operation since 1982 (Follacci, 1987, 1988, 1999). Distance measurements have been regularly acquired and indicate velocities of 1 cm/day on average. Two accelerations have been registered: one in autumn 1987 with velocities greater than 10 cm/day and one at the beginning of 1997 with velocities greater than 5 cm/day (Follacci, 1999). Moreover, these measurements reveal a seasonal response of the landslide characterised by an acceleration of movements correlated to snow melting (Follacci, 1987, 1999). For a few years, this distance monitoring has been combined with other types of investigations: hydrogeological studies (Compagnon et al., 1997; Guglielmi et al., 2000; Cappa et al., 2004), remote sensing (Casson et al., 2003; Squarzoni et al., 2003) and subsurface geophysical investigations (Lebourg et al., 2005; Jomard et al., 2007a,b). Different types of geometric, mechanic or hydromechanic models have been derived from these data sets (Merrien-Soukatchoff et al., 2001; Cappa et al., 2004) but none of them visualise the morphology of the main slip surface geometry. However, Jomard et al. (2007a) have recently investigated, using electrical methods, the vertical structure of the upper part of the NE lobe of the La Clapière landslide. Their

results show a very strong decrease in the resistivity to a depth of approximately 90 m which could be associated with the main shear surface of this landslide at this altitude.

The slope of the unstable zone is about 37°, but is not constant along the profile: the low part of the slope is steeper than the high part. The change of gradient corresponds to the limit of extension of quaternary glaciers, as it is frequent in the alpine valleys (Monterin, 1930; Federici and Pappalardo, 1995; Ballantyne, 2002; Gunzburger et al., 2002; Jomard, 2006). The slope can be separated into three entities: a stable internal zone where foliation has a strong dip varying from 60° to 80° towards the interiors of the slope, a zone of approximately 200 m thickness where foliation is gradually tipped to horizontal, the slipped zone where displacements towards the valley are significant. The surface of the landslide is quite irregular because of numerous rock-fall accumulation, tilted terraces and internal cracks.

In this area, the basement unit is composed of migmatitic paragneisses (Anelle Formation) and orthogneisses (Iglière Formation) bearing a strong Hercynian foliation (Fig. 2) (Follacci, 1987; Follacci et al., 1988). This foliation is normally oriented 115° E, 70° NE but, in the La Clapière area, it is progressively rotated to a subhorizontal attitude by
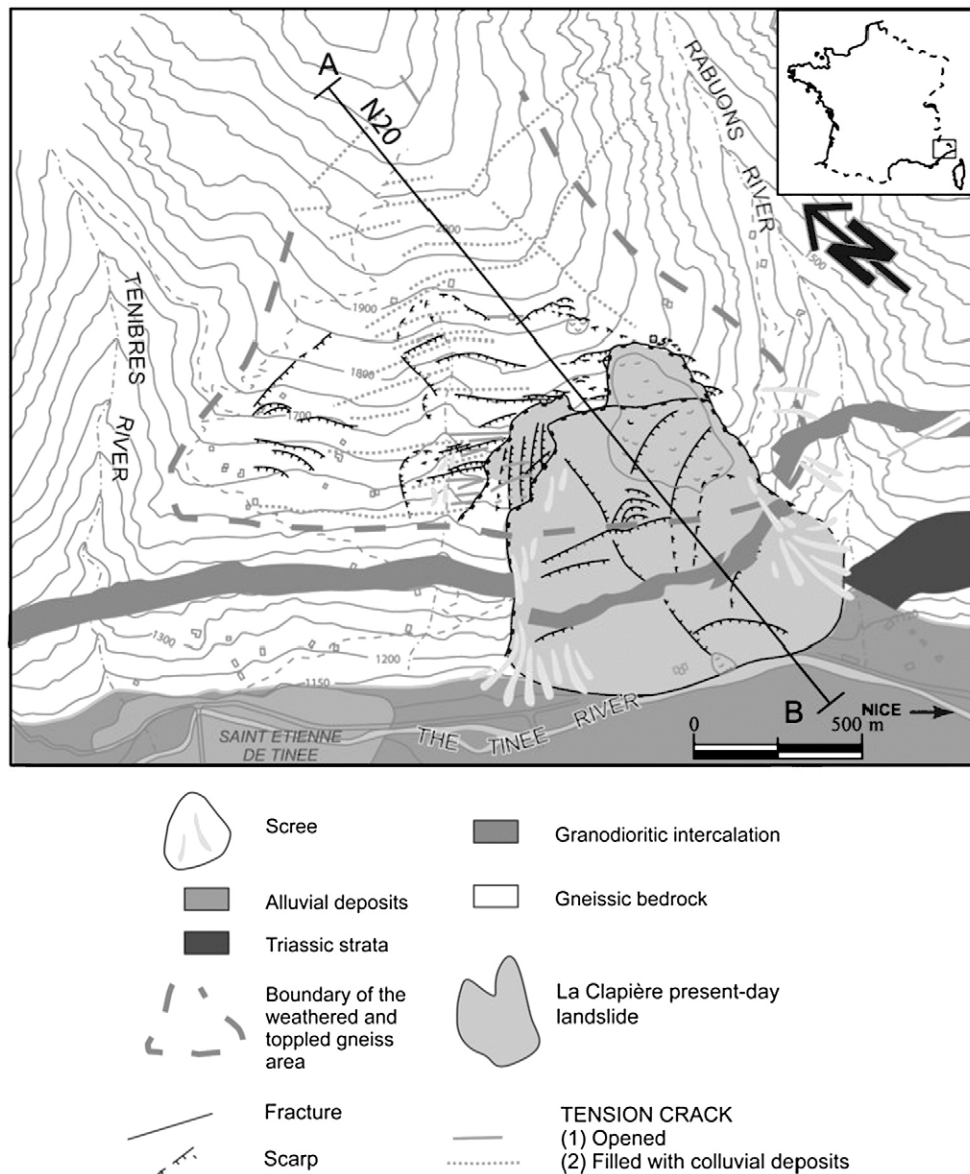
Fig. 2. Geomorphological context of the La Clapière landslide from Cappa et al., 2004. The line AB corresponds to the cross section used to represent the 2D geometry model (see Fig. 3).

a structure called the La Clapière fold (Fabbri and Cappa, 2001; Gunzburger and Laumonier, 2002). The axis of the fold is 120° E, 15° NW; the axial plane is 140° E, 40° SW. The La Clapière landslide occurs in the upper/short limb of the fold.

Two origins of the La Clapière fold are currently proposed. It is either tectonic (Gunzburger and Laumonier, 2002; Delteil et al., 2003) or gravitational (Follacci, 1987). However, the numerical approach conducted by Merrien-Soukatchoff et al. (2001) shows that the gravitational toppling proposed by Follacci (1987) must be reconsidered.

The "La Clapière" slope itself is affected by many tectonic discontinuities. A complete description can be read in Guglielmi et al. (2000), Gunzburger and Laumonier (2002) and Cappa et al. (2004). The major fractures are subvertical N20 faults intersecting the whole slope far from the active landslide and limiting several parallels, a few hundred meters wide, N20 slices. The displacements measured via the monitoring system have also on average an N20 orientation (Guglielmi et al., 2002). Thus, it can be stated that faults play the rule of "tracks" for deformations. For this reason, numerical modelling was not undertaken on a real three-dimensional (3D) slope topography but only with a two-dimensional geometry representing

one N20 slice limited on both sides by N20 accidents with no normal displacements (plane strain model). This choice is identical to those taken by Merrien-Soukatchoff et al. (2001) and Gunzburger et al. (2002). It gives an optimistic view of reality since it leads to consideration of the slope as infinite in its third dimension. In fact, the presence of Rabuons and Ténibres valleys suggests an absence of lateral clamping of the slope which could lead to alternative testing of plan stress conditions.

Cappa et al. (2004) have numerically tested the influence of the location and the amount of water infiltration on the hydromechanical behaviour of La Clapière slope. Their results showed that the most destabilising area is located in the middle part of the slope. However, due to the internal complexity of the slope hydrogeology, especially the existing perched aquifer in the decompression toppled zone directly connected to the landslide, the most dangerous infiltration inflow is not necessarily that on the landslide area.

The first studies of the La Clapière landslide were carried out in 1977. Distance measurements have been regularly acquired since 1982. These data indicate velocities of 1 cm/day on average. Two accelerations have been registered: one in autumn 1987 with velocities greater than

10 cm/day and one at the beginning of 1997 with velocities greater than 5 cm/day (Follacci, 1999). Moreover, these measurements reveal a seasonal response of the landslide characterised by an acceleration of movements correlated to snow melting (Follacci, 1987, 1999). For a few years, this distance monitoring has been combined with other types of investigations: hydrogeological studies (Compagnon et al., 1997; Guglielmi et al., 2000), remote sensing (Casson et al., 2003; Squarzoni et al., 2003) and subsurface geophysical investigations (Jomard et al., 2007a,b). Different types of geometric, mechanic or hydromechanic models have been derived from these data sets (Merrien-Soukatchoff et al., 2001; Cappa et al., 2004) but none of them visualise the morphology of the main slip surface geometry. Based on cross-sectional geometry, the depth of the failure surface may not exceed 100–200 m (Fig. 2 in Cappa et al., 2004), but no data exist to confirm this estimation. In this study we present the 2D morphology and the image of the slip surface of the La Clapière landslide.

3. Mechanical modelling

The 2D numerical modelling of the "La Clapière" landslide has been done with the ADELI numerical code developed by R. Hassani and J. Chery (Hassani, 1994; Hassani et al., 1997). This code has been developed to model the subduction process of the lithosphere (Hassani et al., 1997; Bonnardot et al., 2008). Different rheological laws can be considered including elasticity and elastoplasticity.

The time evolution of the model is governed by a quasi-static problem which consists finding the vector field $v: \Omega \to R^2$ and the symetric tensor field $\sigma: \Omega \to R^2$ satisfying:

$$\begin{cases} div\sigma + \rho g = 0 \text{ in } \Omega \\ \dfrac{D\sigma}{Dt} = G(\sigma, d) \text{ in } \Omega \\ \text{with boundary conditions} \end{cases}$$

where Ω is the physical domain at time t, σ is the Cauchy stress tensor, v is the velocity vector, g is the acceleration vector due to gravity, ρ is the rock density and $d = \frac{1}{2}(\nabla v + \nabla v^T)$ is the Eulerian strain rate tensor. The functional G stands for a général constitutive law. In this code, beyond elastic domain, three regimes of rock behaviour can be considered: brittle, semibrittle and ductile.

In the elastic domain the constitutive law is simply given by

$$G(\sigma, d) = 2\Gamma d + \lambda \text{tr}(d)I$$

where λ and Γ are the Lamé parameters, I is the identity tensor and tr trace operator. Value of Young's modulus and Poisson's ratio are given in the next part of this paper.

In order to mimic a pressure dependent yield strength we use the elastoplastic Drucker–Prager model (Desai and Siriwardane, 1984) for which the yield function is given by:

$$F(\sigma) = J_2'(\sigma) + \alpha J_1(\sigma) - \alpha P_o$$

with $J_2'(\sigma) = [(3/2 \, s{:}s)]^{1/2}$ the second invariant of the deviatoric stress s, $J_1(\sigma) = (1/3)\sigma{:}I$ the mean pressure and

$$\alpha = \frac{6\sin\phi'}{3 - \sin\phi'}, P_o = c'/\tan\phi'$$

where c' is the cohesion and ϕ' the friction angle.

This code is based on a finite element method for space discretization associated with a dynamic relaxation method for the discretization. This method is described in Hassani et al., 1997, and leads to a set of non-linear equations:

$$M\ddot{u} = F_{int}(u, \dot{u}, t) + F_{ext}(u, t) + F_c(u, \dot{u}, t)$$

where the vectors F_{int} and F_{ext} are the internal and external nodal forces, F_c is the vector of contact reaction, u, $\dot{u}$ and $\ddot{u}$ are the vectors of nodal displacements, nodal velocities, and nodal accelerations, respectively. M is a fictitious mass matrix. The quasi-static solution is reached when the inertial regularising term $M\ddot{u}$ is negligible compared to the external forces. The numerical divergence of the result means that failure appears and involves a destabilising of the solid mass.

For each numerical experiment presented in this work, several mesh have been tested (6000, 10,000, 15,000 and 20,000 elements) and 5×10^4 to 1×10^6 time steps were used for a total duration of 100 or 10,000 years to check the numerical accuracy. The lengths of the time steps are then 52 min to 17 h for the duration of 100 years, and 87 h to 72 days for the duration of 10,000 years.

3.1. Geometry and boundary conditions

The geometry used is two-dimensional. The initial state topography is taken from the oldest available map (dated from 1933) in order to eliminate as far as possible recent slope deformations. The velocity boundary conditions are shown in Fig. 3. Gravity is the only force.

3.2. Mechanical parameters

The "La Clapière" slope is constituted of migmatitic paragneisses and migmatitic orthogneisses (Follacci et al., 1988; Fabbri and Cappa, 2001; Gunzburger and Laumonier, 2002). Those rocks bear a strong Hercynian foliation, and are therefore highly anisotropic. However, numerical modelling has first been undertaken with isotropic rheological properties. The rocks are also affected by a great number of fractures of various scales and origins, which play a major rule in rock mass strength deterioration and deformability increase. To take them into account, one method consists of homogenising the rock mass by using the Rock Mass Rating (RMR) methodology (Bieniawski, 1989; Gunzburger and Merrien-Soukatchoff, 2002; Gunzburger et al., 2002; Aydin and Basu, 2005) to provide an Equivalent Continuous Medium (ECM). Rock mass classification is a means for the evaluation of the performance of rock cut slopes based on the most important inherent and structural parameters. The factors related to the general condition of rock mass and the condition and geometric characteristic of discontinuities constitute the base of the existing classification systems. The most commonly used factors are (a) the intact rock strength, (b) the Rock Quality Designation (RQD) index, (c) the condition of discontinuities, (d) the spacing of discontinuities and (e) the groundwater outflows. It is worth mentioning that these factors comprise the five rating elements which form the fundamental RMR system initially developed for underground structures (Bieniawski,
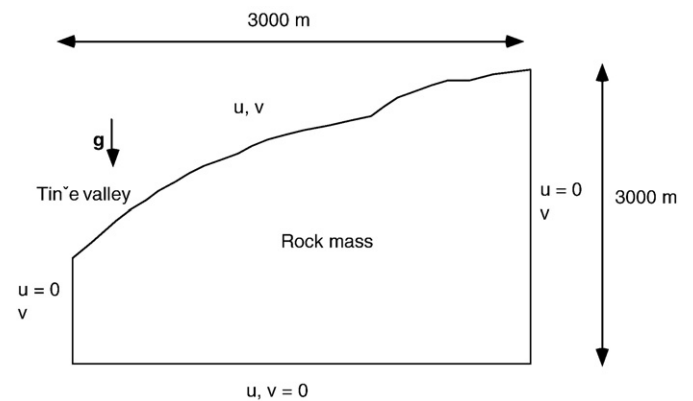

Fig. 3. Geometry of the model and boundary conditions. This geometry is associated to the cross section AB drawing in Fig. 2. u and v are the horizontal and vertical component of the velocity respectively. Only the gravity force (g) is present.

1989). From a statistically representative number of measures of fracture orientation, estimation of Joint roughness coefficient (JRC; Barton, 1976) and joint compressive strength (JCS) field assessment perform on a large number of discontinuities through simple equipment (pocket shape tracer and Schmidt hammer) and empirical correlations (Hoek and Brown, 1980; Bieniawski, 1989) the most important geomechanical properties of the rock mass.

The mechanical parameters of the ECM obtained by this approach for the "La Clapière" site are: Young's Modulus, $E = 6.4$ MPa, cohesion, $c' = 210$ kPa, angle of internal friction, $\phi' = 29°$, Poisson's ratio, $\nu = 0.3$ and density, $\rho = 2400$ kg/m³ (Gunzburger, 2001; Gunzburger and Merrien-Soukatchoff, 2002):

These parameters are considered in our study as the reference parameters. In our numerical approach, we model the mechanical behaviour using an elastoplastic pressure dependent law for which the failure criterion is the Drucker–Prager one (Desai and Siriwardane, 1984). We consider in this study a homogeneous rock mass in which heterogeneities such as the Iglière formation can be considered.

Of the five parameters given previously, two have been tested systematically: the cohesion (c') and the friction angle (ϕ'). The others were kept constant.

Four tests have been performed.

– Test 1: We tested the couple (c', ϕ') from the reference couple (210 kPa, 29°) in order to determine the critical couple for which the destabilisation appears.
– Test 2: The cohesion (c') is constant and we sought the critical value of ϕ'.
– Test 3: The friction angle is constant and we sought the critical value of c'.
– Test 4: Influence of the Iglière formation

4. Numerical results

The results of the test 1 are given in Table 1. They are identical whatever the mesh used, and the duration applied. They show a critical couple (c', ϕ') equal to 70.0% of the reference couple, i.e. (1.47 10^5 Pa, 20.3°) with which the numerical solution does not converge (Table 1).

All the converged solutions, which correspond consequently to a static solution, are characterised by three plastic deformation zones. The first one is located at the base of the slope up to 1400 m in altitude and at a depth of about 200 m (Fig. 4a). The second one is located along the slope between 1400 m and 1800 m of altitude and below the surface (about 50–100 m). The third zone is at the top of the slope (Fig. 4a). When the couple (c', ϕ') is equal or lower to the critical couple, the divergence of the numerical experiment is due to a strong plastic deformation located at the bottom of the slope (Fig. 4b). This plastic deformation leads to the destabilisation of the massif by a regressive evolution of the landslide from the bottom to the top of the slope. This deformation extends up to 1800 m, which is actually the top of the "La Clapière" landslide. This progression of the deformation only concerns a depth of around 150 ± 50 m like a channel of deformation. It is interesting to note that the two altitudes given previously (1400, 1800 m) correspond to a change of the slope in the
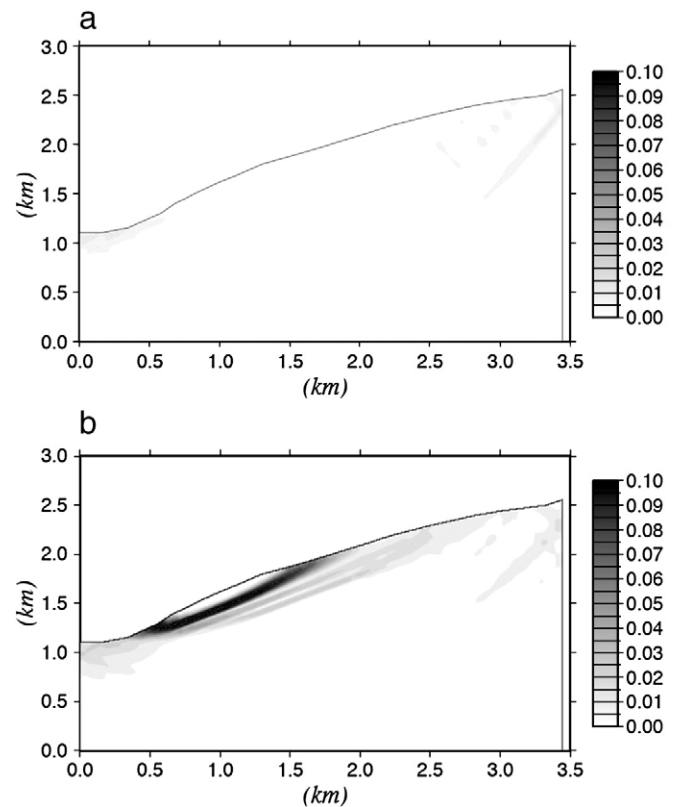

Fig. 4. Cumulated plastic deformation obtained for two simulations (Test 1). The scale is fixed to a maximum of 0.1 cumulated plastic deformation in order to compare with other numerical results: (a) the couple (c', ϕ') corresponds to the reference couple (100%, 210 kPa, 29°). The solution is converged. The maximum of cumulated plastic deformation (c.p.def.) is equal to 0.02 in this run. (b) The couple corresponds to 70% (147 kPa, 20.3°) of the reference couple. The solution is not converged. The maximum of cumulated plastic deformation is equal to 1.4.

topography of 1933. Do these results suggest that the distribution and the temporal evolution of the deformation are controlled by these changes in the slope? The question remains open and deserves to be studied in more detail.

All the results obtained in the different tests are summarised in Table 2. We observe that the instability seems to be mainly controlled by the friction angle. Indeed, when the cohesion is kept constant and equal to 210 kPa, the divergence of the calculation is observed from an internal friction angle value of the same order to those obtained when the variable is the couple (c', ϕ'). When internal friction is kept constant, the divergence is never obtained. The result obtained for ($c' = 0$ kPa, $\phi' = 29°$) is shown in Fig. 5. We can observe that plastic deformation is located only at the surface between the foot of the actual landslide and the altitude 1800 m.

Test 4 takes account of the presence of the Iglière formation which is located between 1400 m and 1450 m in altitude. Our goal here was to show the influence of the Iglière formation on the propagation of the deformation. We tested different cases in which the mechanical parameters (c' and ϕ') of the Iglière formation were modified compared to those of the remainder of the solid mass. Thus, if we

Table 1
Numerical results for test 1.

c' (kPa), ϕ'	% of the reference couple	Numerical solution
210, 29.0°	100	Convergence
189, 26.1°	90	Convergence
168, 23.2°	80	Convergence
153.3, 21.17°	73	Convergence
147, 20.3°	70	Divergence
136.5, 18.85°	65	Divergence

Table 2
Results of the numerical experiments for the three tests.

Test	Constant	Variable	Numerical solution	
			Convergence	Divergence
1		(c', ϕ')	≥73%	≤70%
2	c'	ϕ'	≥70%	≤67%
3	ϕ'	c'	>0%	Never
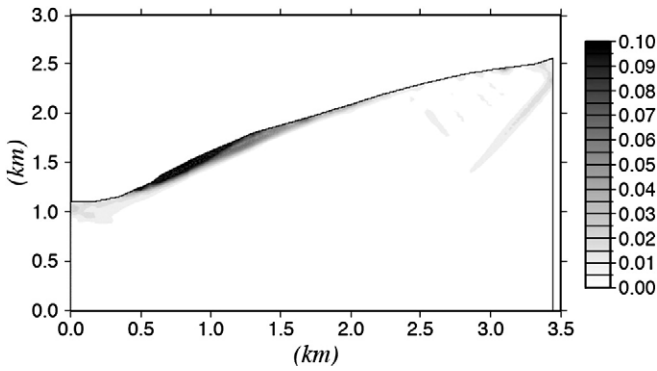
Fig. 5. Cumulated plastic deformation obtained for one simulation corresponding to Test 2 with cohesion equal to 0 Pa and $\phi' = 29°$. The maximum of c.p.def. is equal to 0.93 in this run, but the scale has been limited to. 0.1 in order to compare with other results.

keep the mechanical parameter of the solid mass equal to the reference case (210 kPa, 29°) and those of the Iglière formation equal to 120%, or 150%, we observe that the deformation initiates progressively at between 1100 and 1300 meters and extends gradually upstream, reaching a depth of 150 m under the surface. The deformation can also be completely stopped at the base of the Iglière formation as soon as its mechanical parameters are greater than 150% of the reference case (Fig. 6a). In this case, the channel of deformation no longer exists and deformation is concentrated between the foot of the slope and the Iglière formation. Now, if the mechanical parameters of the Iglière formation are lower than the solid mass (80%, 70%) we obtain results comparable to those obtained in Test 1 (Fig. 6b).

Finally, if we keep the mechanical parameters of the Iglière formation equal to 100% of the reference case and modify those of the solid mass, we obtain the same critical value for the divergence of the run as that observed in test 1, i.e. for a value lower than 70% of the reference case, but the distribution of plastic deformation is different (Fig. 7a). We observe a strong plastic deformation at the foot of the slope associated with a gravitational toppling of the Iglière formation. Above it, the massif shows a large and deep distribution of deformation that reaches the surface and leads to a slope-rupture at about 1800 m which corresponds exactly to the current situation of the La Clapière landslide (Fig. 7b, c). On the site, we do indeed observe at different altitudes, between 2000 m and 2500 m, several cracks (Jomard, 2006) which could be related to the plastic deformation lineaments that we observe on our numerical results (Fig. 7a). We are well aware that we cannot prove this hypothesis but the correlation is striking.

5. Geophysical investigation

Investigation into the geometry of landslides using geophysical prospecting methods can be carried out by using a wide set of techniques, among which seismic and geoelectrical methods are the most widely adopted. Seismic methods directly investigate mechanical parameters, but due to the high mechanical energy attenuation of

Table 3
Results of the Vertical Electrical Sounding obtained with Schlumberger array (see Fig. 10).

Site	Site's altitude	AB/2	Rho$_1$ (Ω m)	Rho$_2$ (Ω m)	Rho$_3$ (Ω m)	Rho$_4$ (Ω m)	H$_1$ (m)	H$_2$ (m)	H$_3$ (m)
G1	1445	193	2274	1484	4126	–	6.9	110	–
G2	1305	193	1244	12,105	1353	38	2.5	0.9	81.0
G3	1250	193	5669	1272	218	–	5.5	39.7	–
G4	1160	373	1455	3611	388	–	0.5	20	–
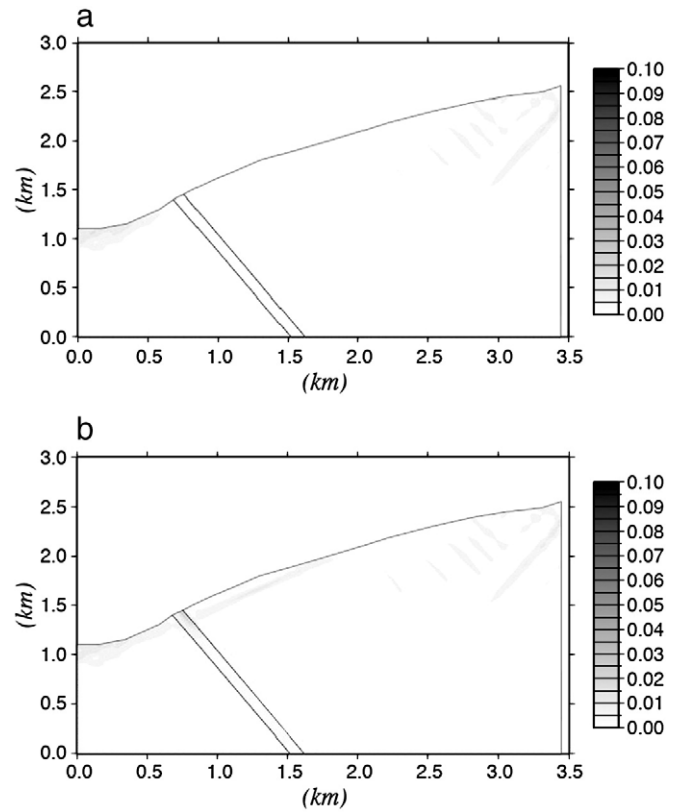
Fig. 6. Cumulated plastic deformation obtained for simulations corresponding to Test 4 which takes account the Iglière formation. (a) The solution is converged and has been obtained for mechanical parameters (c', ϕ') of the Iglière formation equal to 150% of the reference case. The mechanical parameters of the massif are equal to the reference case. The maximum of c.p.def. Is equal to 0.032. (b) The solution is converged and corresponds to the mechanical parameters (c', ϕ') of the Iglière formation equal to 70%. The mechanical parameters of the massif are equal to the reference case. The maximum of c.p.def. is equal to 0.47.

weathered rock on the La Clapière landslide, it needs very strong energy sources. The electrical resistivity method instead may constitute the best compromise between cost (time and money) and research needs. Thus, in order to study the shallow structures involved in the mass movement, 1D and 2D geoelectrical prospections were carried out.

Four Vertical Electrical Soundings (VES) were performed at different altitudes using a Schlumberger array. Soundings were made with a minimum AB/E of 193 m. These four VES were performed almost perpendicular to the longitudinal axis of the landslide body (Fig. 1). These data were acquired using a Syscal resistivimeter from Iris Instruments Ltd.

The protocol used for Electrical Resistivity Tomography (ERT) in this study was previously tested in Jomard et al. (2007a,b). The key acquisition and inversion parameters are as following. Measurements were undertaken with a multielectrode 2D device, using the Syscal R1 Plus imaging system (IRIS Instrument). The 2D devices are constituted by 48 electrodes separated by 10 m (limit of the system). This approach was undertaken with a multielectrode 2D device, using 48 electrodes separated by 10 m. We systematically used a pole–pole and dipole–dipole array, with measurement frequency of 4 Hz, for about 800 to 1100 measurements for each profile. The 2D resistivity data were recorded using the Syscal R1 Plus imaging system (IRIS Instrument). The data are classically presented in the form of pseudo-sections (Edwards, 1977), which give an approximate picture of the subsurface resistivity. The data, once recorded, are transferred to and processed on a computer. Inversion of the data is required to obtain a vertical true resistivity section through the underlying structure (Loke and Barker, 1996; Bear, 1996). The field data depicted as contoured pseudoresistivity sections
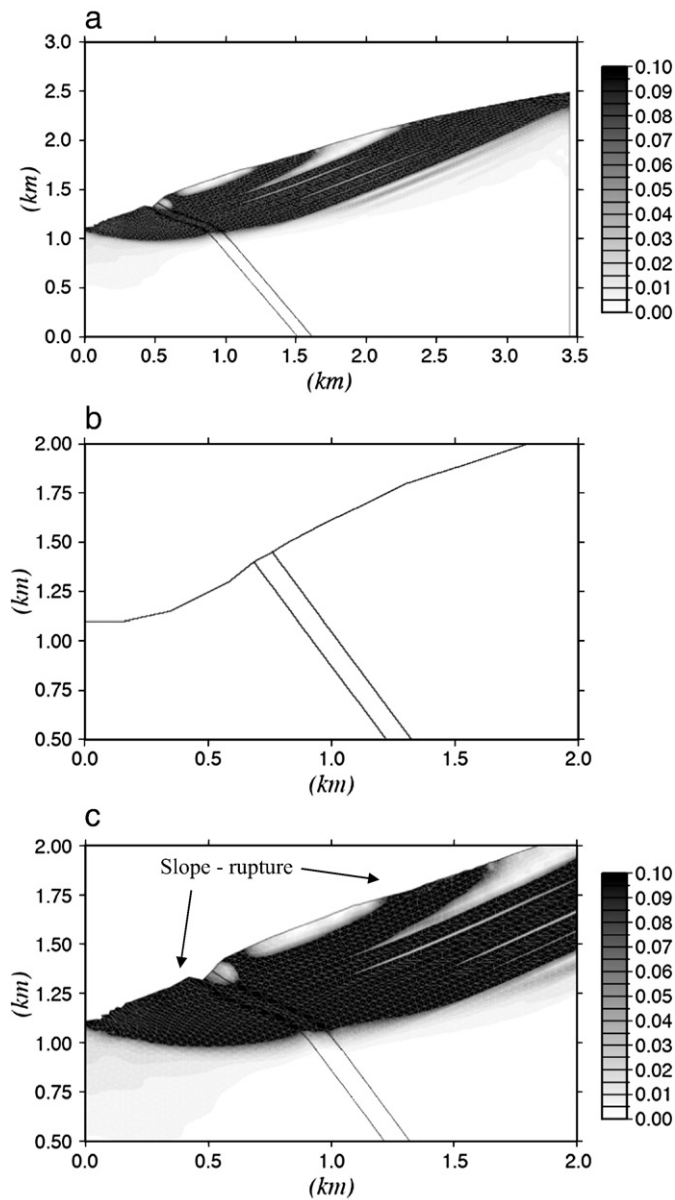
Fig. 7. Cumulated plastic deformation obtained for simulation corresponding to Test 4. a) The mechanical parameters (c', ϕ') of the Iglière formation are equal to 100% and those of the massif equal to 70% of the reference case. The maximum of c.p.def. is equal to 2.4. The solution diverges (b) corresponds to a focus at the beginning of the run. c) is obtained just before the divergence of the run.

were inverted with the RES$_{2D}$INV software written by Loke (1997). Furthermore, the constraints provided by the topographic variations have been introduced into the inversion processing. To reduce the error on the resistivity interpretation, we systematically correlated each electrode to geological field observations. The interpretation of the resistivity cross section must be improved by a high resolution geological and structural study. This last aspect reduces the error of the interpretation.

5.1. VES results

The data were inverted with R1X software using horizontal layer models. Data inversion allowed us to identify:

a) A main upper layer which is found in each interpretative model of the four VES (Fig. 8). It is constituted by (1) a weathered and

fractured upper part whose resistivity is not very clearly shown due to the small amount of experiment data belonging to the beginning of the ρ_{app}(AB/2) curves; (2) a more homogeneous body whose depth increases as a function of the site altitude.

b) A shallower interface which corresponds to the top of a more conductive layer. The resistivity of this layer is at least 10 times weaker than that of the upper layer except for profile G1 (1445 m) for which the resistivity increases slightly (by a factor of 3). However, for this profile the increase is characterised by only two points. If we consider it as significant, they could be associated with a local heterogeneity. From these VES we can propose an electrostratigraphic schema which is shown in Fig. 9.

5.2. Comparison with the pole–pole electrical profile obtained by Jomard et al. (2007a,b)

In 2007, Jomard et al. (2007a) obtained an electrical tomography profile at the top of the La Clapière landslide. The altitude of this profile was 1650 m. This profile is shown in Fig. 10. If we extract from our analyse the upper part of the profile (0 to 20–30 m) which corresponds to the unstable part studied by Jomard et al. (2007a,b), we observe an electrical vertical distribution characterised by two layers. The first one is about 90 m in thickness and characterised by high resistivity ($\geq 5000\ \Omega$ m). The second is associated with very low resistivities ($\leq 150\ \Omega$ m). This stratification in resistivity is in good agreement with the SEV results presented previously. All these results, other than the profile SEV-G1, show the presence of a strong resistivity gradient which delimits two zones (Figs. 9 and 10a). An upper part which could be associated with the principal structure of the La Clapière landslide and a lower part which could correspond to a saturated material, or possibly to the perched aquifer as suggested by Guglielmi et al. (2002) and Cappa et al. (2004). The boundary between these two parts could be associated with the main shear surface of the La Clapière landslide (Fig. 10b).

6. Discussion and conclusions

Different mechanical numerical models have been performed to better locate the deformation in the rock mass and determine critical geomechanical parameters from which the landslide occurs in the specific case of "La Clapière". We have used geomechanical parameters obtained by Gunzburger (2001) using a RMR methodology. Although the solid mass was regarded as mechanically homogeneous and in spite the simplicity of our model, our numerical simulations reproduce very well the La Clapière landslide. The deformation leads to the destabilisation of the massif by a regressive evolution of the landslide from the bottom to the top of the slope. The destabilisation is initiated in our simulation from a cohesion value lower than 0.153 MPa which is very close to the value of 0.2 MPa determined using the RMR methodology by Gunzburger (2001) and those obtained from La Clapière material by triaxial tests by Jomard et al. (2007a,b) which show a decreasing effective cohesion between 0.036 MPa and 0.002 MPa.

All simulations reveal a good correlation between the calculated deformation and the current morphology of the slope. In both cases, the disorders are for an altitude ranging between 1100 m and 1800 m and with a maximum deformation located at the bottom of slope. When we introduce structural and mechanical heterogeneities with the Iglières formation the destabilisation is still observed, but the deformation is associated with a folded structure as we can see in Fig. 7c. This toppling is a structural characteristic of La Clapière landslide and its origin was discussed a long time (Follacci, 1987; Gunzburger and Laumonier, 2002; Delteil et al., 2003; Jomard, 2006). If the scientific community seems to be agree with the fact that the folded structure has a tectonic origin, it is not evident to say that fold structure has not direct link with current slope instability as suggested
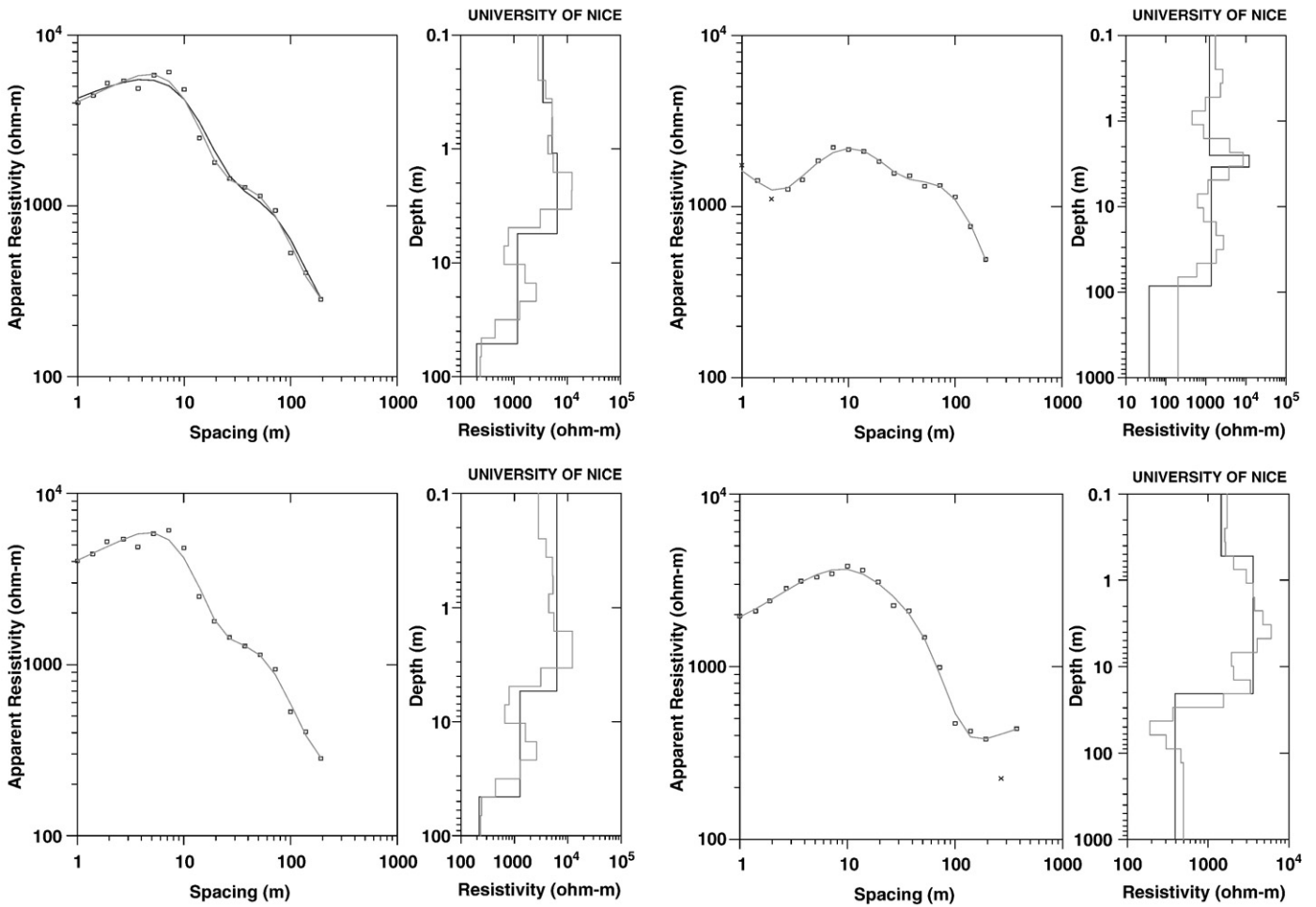
Fig. 8. Vertical Electrical Soundings (SEV) obtained on the La Clapière landslide. a) SEV G1: 1445 m in altitude, b) SEV G2: 1305 m, c) SEV G3: 1250 m, d) SEV G4: 1160 m.

by Gunzburger and Laumonier (2002). Indeed, our study shows that coupling between mechanic "weathering" parameters and gravity is sufficient to cause a destabilisation of the solid mass with a folded signature.

The instability process is associated with a large and more and less deep distribution of deformation in which the slope topography seems to be a key parameter. The reported simulations suggest that changes of the slope "drive" the diffusion of the plastic deformation,
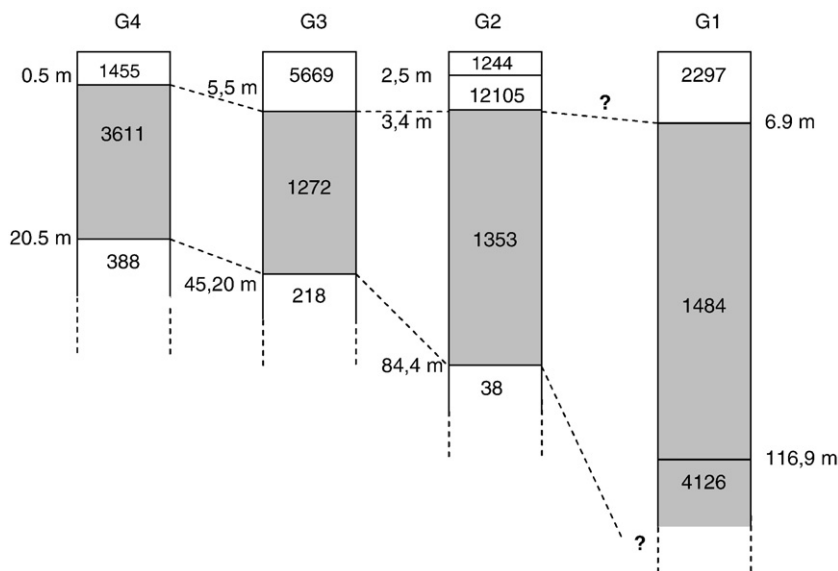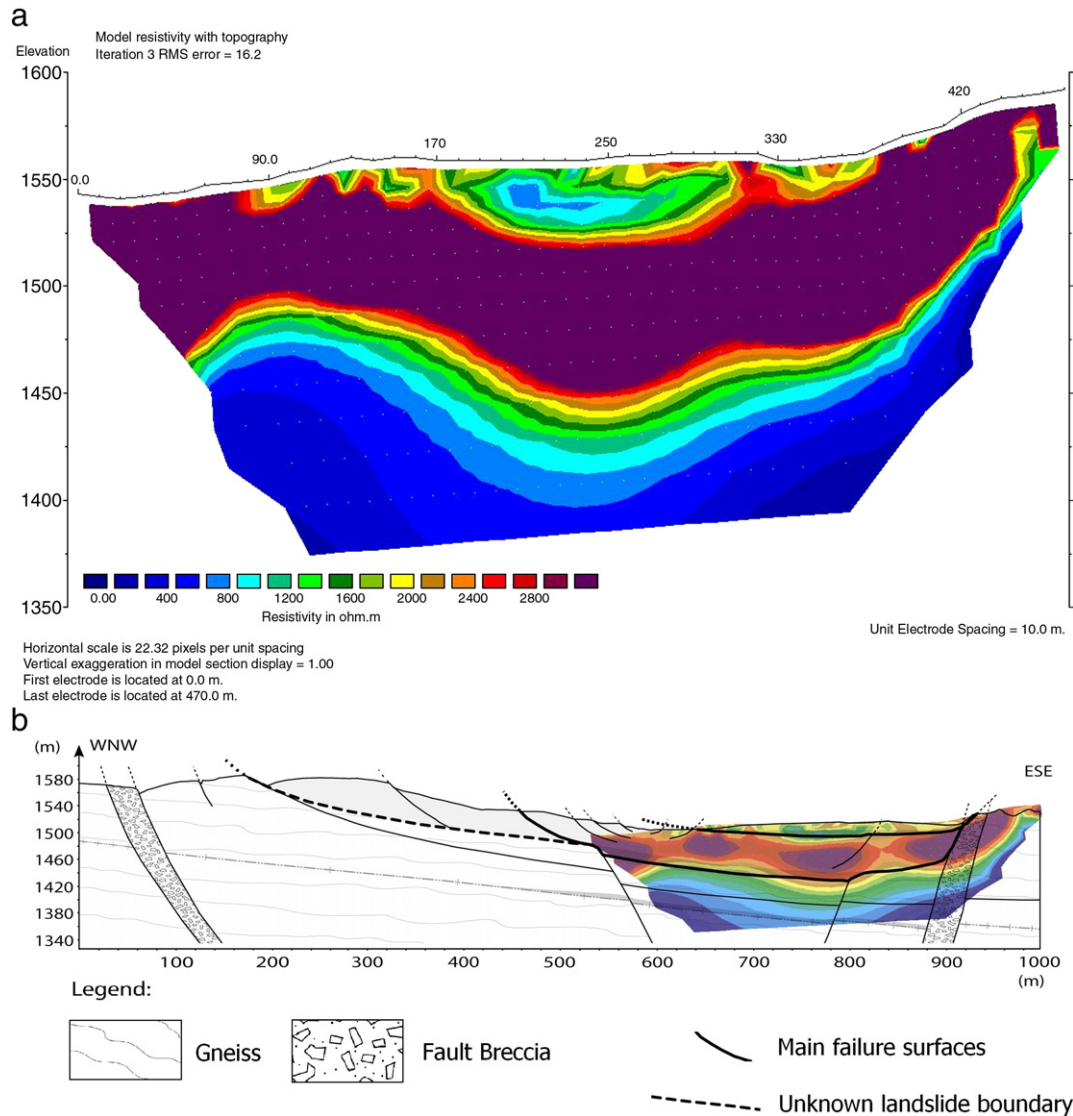

Fig. 9. Electrostratigraphic synthesis obtained from SEV presented in Fig. 8 and Table 3. See location of SEV G1, G2, G3 and G4 in Fig. 1.

Fig. 10. (a) Electrical Resistivity Tomography (ERT) obtained at the top of the landslide from Jomard et al. (2007a) and his geological interpretation. We observe three electrical structures: (1) the unstable part between 0 and 20–30 m of depth, (2) a layer of about 90 m thick which could correspond to the principal structure of La Clapière and (3) a perched aquifer as suggested by Guglielmi et al. (2002) and Cappa et al. (2004). (b) ERT projection on geological cross sections.
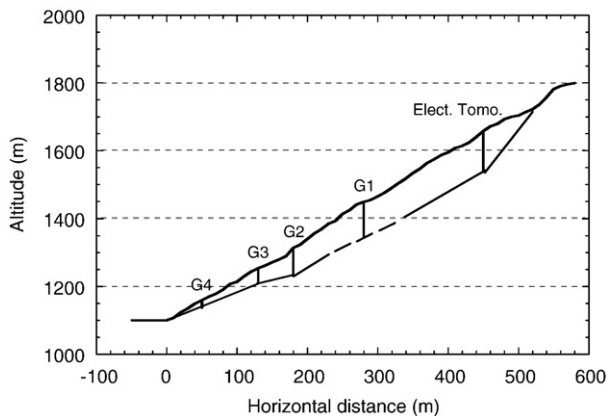
Fig. 11. Synthesis of the electrical results obtained on the La Clapière landslide. These results enable the mean shear surface to be established at between 50 and 150 m in depth in the solid mass of the La Clapière landslide.

possibly through a channel of deformation. This channel could be then the privileged zone along which the fracture is initiated. In our numerical results the depth of this channel is between 80 and 120 m according to the altitude.

It is in this goal that we have performed 1D and 2D electrical study at different altitude. All our geophysical results clearly show two superposed layers characterised by a strong decrease in resistivity at depth. These data are very well correlated with 2D electrical tomography obtained by Jomard et al. (2007a,b) and strongly suggest that electrical gradient is associated with the main shear surface of the La Clapière landslide. The compilation of these data allowed us to give for the first time a cross section of the actual La Clapière landslide (Fig. 11). From this figure we can exclude an obvious correspondence between the channel deformation obtained by numerical approach and the main shear surface suggested by electrical data. This good correlation between numerical and electrical results is in agreement with the destabilisation process proposed by Guglielmi et al. (2005). The presence of penetrative tectonic faults favours water infiltration and consequently a deep weathering of the rock. The modification of the mechanical parameters coupled with gravitation can induce a partial destabilisation of the massif to a depth about 120 m. As a

function of the weather, the perched aquifer identified by Guglielmi et al. (2002) and Guglielmi et al. (2005)\ and slope drainage should accelerate the destabilisation process. Thus, the destabilisation area could be much larger than the current La Clapière landslide with a spatial evolution partially control by the changes of the slope, as is suggested by our numerical results.

References

Aydin, A., Basu, A., 2005. The Schmidt hammer in rock material characterization. Engineering Geology 81, 1–14.

Ballantyne, C.K., 2002. Paraglacial geomorphology. Quaternary Sciences Review 21, 1935–2017.

Barton, P., 1976. The shear strength of rock and rock joints. International Journal of Rock Mechanics and Mining Sciences and Geomechanics Abstracts/13, pp. 255–279.

Bieniawski, Z.T., 1989. Engineering Rock Mass Classifications. John Wiley & Sons, New-York. 251 p.

Bonnardot, M.-A., Hassani, R., Tric, E., Ruellan, E., Regnier, M., 2008. 3D mechanical modelling of margin geometries in subduction zones. Geophysical Journal International. doi:10.1111/j.1365-246X.2008.03752.x.

Brueckl, E., Parotidis, M., 2001. Estimation of large-scale mechanical properties of a large landslide on the basis of seismic results. International Journal of Rock Mechanics and Mining Sciences 1365–1369.

Cappa, F., Guglielmi, Y., Soukatchoff, V., Mudry, J., Bertrand, C., Charmoille, A., 2004. Hydromechanical modelling of a large moving rock slope inferred from slope levelling coupled to spring long-term hydrochemical monitoring: example of the La Clapière landslide (Southern Alps, France). Journal of Hydrology 291, 67–90.

Casson, B., Delacourt, C., Baratoux, D., Allemand, P., 2003. Seventeen years of the "La Clapière" landslide evolution analysed from ortho-rectified aerials photographs. Enginerring Geology 123–139.

Compagnon, F., Guglielmi, Y., Mudry, J., Follacci, J.P., Ivaldi, J.P., 1997. Approche chimique et isotopique de l'origine des eaux en transit dans un grand glissement de terrain: exemple du glissement de la Clapière (Alpes-Maritimes). Comptes Rendus de l'Académie des Sciences Paris 325 (II), 565–570.

Delteil, J., Stephan, J.F., Atta, M., 2003. Control of Permian and Triassic faults on Alpine basement deformation in the Argentera massif (external southern French Alps). Bulletin de la Société Géologique de France 174, 55–70.

Desai, C.S., Siriwardane, H.J., 1984. Constitutive Laws for Engineering Materials, With Emphasis on Geologic Materials. Prentice-Hall, Englewood Cliffs New Jersey. 457 pp.

Eberhardt, E., Stead, D., Coggan, J.S., 2004. Numerical analysis of initiation and progressive failure in natural rock slopes — the 1991 Randa rockslide. International Journal of Rock Mechanics and Mining Sciences 41, 69–87.

Eberhardt-Philips, D., Stanley, W.D., Rodriguez, B.D., Lutter, W.J., 1995. Surface seismic and electrical methods to detect fluids related to faulting. Journal of Geophysical Research 100, 12,919–12,936.

Edwards, L.S., 1977. A modified pseudosection for resistivity and induced-polarization. Geophysics 42, 1020–1036.

Fabbri, O., Cappa, F., 2001. Apport de l'analyse structurale à la compréhension de la degradation du glissement de la Clapière, Massif du Mercantour, Alpes Maritimes: S. Spé. Soc. Géol. Fr., 12-1.

Federici, P.R., Pappalardo, M., 1995. L'evoluzione récente dei ghiacciai delli Alpi maritime Vol. 18, 257–269.

Follacci, J.-P., 1987. Les mouvements du versant de la Clapière à Saint-Etienne de Tinée (Alpes-Maritimes). Bulletin des Lab. Des Ponts et Chaussée, vol. 39–54, pp. 150–151. 1987.

Follacci, J.-P., 1999. Seize ans de surveillance du glissement de La Clapière (Alpes Maritimes). Bulletin de Liaisin des Lab. Des ponts et Ch, vol. 220, pp. 35–51. 1999.

Follacci, J.P., Guardia, P., Ivaldi, J.P., 1988. Le glissement de la Clapière (Alpes Maritimes) dans son cadre géodynamique. Landslides, pp. 1323–1327.

Guglielmi, Y., Bertrand, C., Compagnon, F., Follacci, J.-P., Mudry, J., 2000. Acquisition of water chemistry in a mobile fissured basement massif: its role in the hydro-geological knowledge of the La Clapiere landslide (Mercantour massif, southern Alps, France). Journal of Hydrology 229, 138–148.

Guglielmi, Y., Vengeon, J.M., Bertrand, C., Mudry, J., Follacci, J.-P., Giraud, A., 2002. Hydrogeochemistry: an investigation tool to evaluate infiltration into large moving rock masses (case study of La Clapière and Séchilienne alpine landslides). Bulletin of Engineering Geology and the Environment 61 (4), 311–324.

Guglielmi, Y., F., Binet, S., 2005. Coupling between hydrogeology and deformation of mountainous rock slopes: insights from La Clapière area (southern Alps, France). C. R. Geoscience 337, 1154–1163.

Gunzburger, Y., 2001. Apports de l'analyse de la fracturation et de la modélisation numérique à l'étude du versant instable de La Clapière (Saint-Etienne-de-Tinée, Alpes-Maritimes), Mémoire de DEA PAE3S. LAEGO, Ecole des Mines de Nancy (France).

Gunzburger, Y., Laumonier, B., 2002. Origine tectonique du pli supportant le glissement de terrain de La Clapière (Nord-Ouest du massif de l'Argentera-Mercantour, Alpes du Sud, France) d'après l'analyse de la fracturation. C. R. Géosciences 334, 415–422.

Gunzburger, Y., Merrien-Soukatchoff, V., 2002. Caractérisation mécanique d'un versant rocheux instable au moyen du système RMR–Cas de La Clapière (Alpes Maritimes). 5th European Conference on Numerical Methods in Geotechnical Engineering, pp. 4–6. Paris, France, Septembre.

Gunzburger, Y., Merrien-Soukatchoff, V., Guglielmi, Y., 2002. Mechanical influence of the last deglaciation on the initiation of the" La Clapière" slope instability (southern French Alps). 5th European Conference on Numerical Methods in Geotechnical Engineering, pp. 4–6. Paris, France, Septembre.

Hassani, R., 1994. Modélisation numérique de la déformation des systèmes géologiques. Thèse de l'Université de Montpellier II.

Hassani, R., Jongmans, D., Chéry, J., 1997. Study of plate deformation and stress in subduction processes using two-dimensional numerical models. Journal of Geophysical Research 102, 17,951–17,965.

Hoek, E., Brown, E.T., 1980. Underground Excavations in Rock. Institution of Mining and Metallurgy, London. 527pp.

Ivaldi, J.-P., Guardia, P., Follacci, J.-P., Terramorsi, S., 1991. Plis de couverture en échelon et failles de second ordre associés à un décrochement dextre de socle sur le bord nord-ouest de l'Argentera (Alpes-Maritimes, France). Comptes Rendus de l'Académie des Sciences 313, 361–368.

Jomard, H., 2006. Analyse multi-échelles des déformations gravitaires dans le massif de l'Argentera-Mercantour, PhD of Université de Nice Sophia Antipolis (France).

Jomard, H., Lebourg, T., Tric, E., 2007a. Identification of the gravitational discontinuity in weathered gneiss by geophysical survey: La Clapière Landslide (France). Journal of Applied Geophysics 62, 47–57.

Jomard, H., Lebourg, T., Binet, S., Tric, E., Hernandez, M., 2007b. Characterisation of an internal slope movement structure by hydrogeophysical surveying. Terra Nova 19 (1), 48–57.

Lebourg, T., Riss, J., Pirard, J., 2004. Influence of morphological characteristics of heterogeneous moraine formations on their mechanical behaviour using image and statistical analysis. Engineering Geology 73, 37–50.

Lebourg, T., Binet, S., Tric, E., Jomard, H., El Bedoui, S., 2005. Geophysical survey to estimate the 3D sliding surface and the 4D evolution of the water pressure on part of a Deep Seated Landslide. Terra Nova 17, 399–406.

Loke, M.H., 1997. Res2DINV software user's manual.

Loke, M.H., Barker, R.D., 1996. Rapid least-squares inversion of apparent resistivity pseudosections by a quasi-Newton method. Geophysical Prospecting 44, 131–152.

Maffei, A., Martino, S., Prestininzi, A., 2005. From the geological to the numerical model in the analysis of gravity-induced slope deformations: an example from the Central Appennies (Italy). Engineering Geology 78, 215–236.

Merrien-Soukatchoff, V., Quenot, X., Guglielmi, Y., 2001. Modélisation par éléments distincts du phénomène de fauchage gravitaire. Application au glissement de La Clapière (Saint-Etienne de Tinée, Alpes-Maritimes), 95/96, pp. 133–142.

Monterin, U., 1930. Les glaciers dans les alpes maritime. Revue de Géographie Alpine, p. 329–341.

Quenot, X., 2000. Etude du glissement de La Clapière. Modélisation du phénomène de rupture, Mémoire de DEA, DEA PAES3S, Ecole Doctorale PROMEMA. Institut national polytechnique de Lorraine, Nancy (France).

Savage, W.Z., Baum, R.L., Morrissey, M.M., Arndt, B.P., 2000. Finite-element analysis of the Woodway landslide, Washington. U. S. Geological Survey Bulletin 2180, 1–9.

Squarzoni, C., Delacourt, C., Allemand, P., 2003. Nine years of spatial and temporal evolution of the La Valette landslide observed by SAR interferometry. Engineering Geology 68 (1–2), 53–66.